ABL INCLUSION EFFECTS ON ROTOR AIRLOADS SIMULATIONS IN A SHIPBORNE ENVIRONMENT

Gregorio Frassoldati, Leonardo Helicopters, Cascina Costa (VA), Italy
Cristiano Capizzi, Leonardo Helicopters, Cascina Costa (VA), Italy

Abstract

This paper gathers the experience gained in exploring the possible setups for a new computational methodology to evaluate the aerodynamic field on ship decks. With respect to the legacy approach used in Leonardo Helicopters Division, the new workflow tries to erode the conservativism limits assumed on the results by improving the accuracy of the outcomes when estimating transient airloads on helicopter blades during start-up procedures on ship decks. All steps of have been developed to be automatable for industrial applications. The improvement in aerodynamics with respect to the previous study [1] takes into account the Atmospheric Boundary Layer (ABL) in an efficient manner, and compare it with other possible numerical models described in literature. The impact on the blade loads derivating from the ABL is be presented through its effect on the rotor loads during start-up manoeuvres. Taking into account the ABL becomes relevant only as the ship orientation changes towards 90°, and affects the rotor airloads depending on the sea state, on the hull height and on the rotor placement on deck.

1. NOTATION

Hereafter the most used symbols and acronyms can be found listed in alphabetical order.

Symbols:

k	Turbulence kinetic energy [J/kg]
ε	Rate of dissipation [J/kg·s]
ω	Specific rate of dissipation [1/s]
u	Velocity [m/s]
Δt	Timestep [s]
Δx	Differential distance [m]
Ls	Ship overall Length [ft]

Acronyms:

ABL	Atmospheric Boundary Layer
AW	AgustaWestland
BC	Boundary Condition
CFD	Computational Fluid Dynamics
CFL	Courant-Friedrichs-Lewy
ISA	International Standard Atmosphere
LES	Large Eddy Simulation
LHD	Leonardo Helicopters Division
RANS	Reynolds-Averaged Navier-Stokes
SBES	Stress-Blended Eddy Simulation
SDR	Specific Dissipation Rate
SFS	Simple Frigate Shape
SFS2	Simple Frigate Shape (2nd version)
SL	Sea Level
SRS	Scale Resolving Simulation
TBL	Turbulent Boundary Layer
TKE	Turbulent Kinetic Energy
TVR	Turbulent Viscosity Ratio

2. INTRODUCTION

Ship operations represents a most demanding scenario for rotorcrafts. Looking at certification by simulation, being able to properly capture the conditions limiting an aircraft's operational capabilities becomes a requirement. This study represents a step in that direction, aiming to describe a computational methodology to evaluate the aerodynamic field on ship decks under the influence of atmospheric boundary layer. In particular, to assess the description that most suits the requirements, the evaluation is based on the impact on rotor loads applications during start-up manoeuvres.

Most times, technical analyses are subject to the pace given by the program management: from there comes a preponderant need for an efficiency tradeoff.

The bluff-body separations taking place downstream of the elements on deck, along with vortices interactions, make the problem a most specific and case-dependent one for a helicopters operational environment. The aerodynamic methodology described in [1] enlightens the best way to overcome legacy approach limitations.

However, to take the accuracy a step further, and without excessively aggravating the computational cost, the revised methodology will try to model the contribution of Atmospheric Boundary Layer (ABL) in two different ways, once again aiming at closing the gap with real world conditions experienced at sea [2] [3].

3. PROBLEM DESCRIPTION

3.1. Reference case study

Several studies, among which [4] and [5], tried to assess the problem correlating wind tunnel experimental campaigns with computational fluid dynamics simulations. Most of the available results provide resourceful insights for literature ship models, such as the SFS2 chosen for this study [Figure 1]. Naturally, this investigation has the objective to find general guidelines to approach the study of an arbitrarily shaped ship as much as possible.

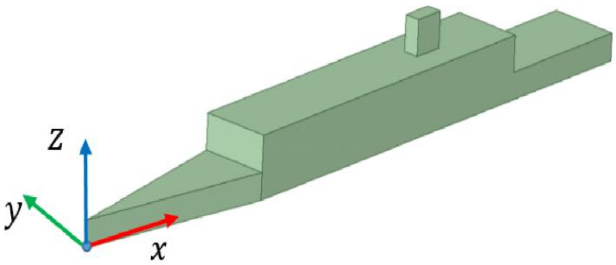

Figure 1: SFS2 model

Naval ship operations are often demanding for helicopters as clearly demonstrated in [6] and [7], and the effects they have on helicopters design influence different aspects of their operational life. For landing manoeuvres, described in [8], as well as for rotor startup procedures, the turbulent airwake is utterly impacting on deck: from there originates the need to assess frequency contents, topological aspects of the wake and the interactions with the aircraft aerodynamics. For this reason, the possible CFD setups in literature explored different possibilities for SRS; the present study takes into account different promising possibilities, as in [9], [10] and [11].

Naturally, the unsteady flow field peculiarities vary depending on the ship geometry, as well as with the relative angle between the ship orientation and the incoming wind. Moreover, the sea state is yet another relevant degree of freedom both for ship attitude and wind speed.

For sake of simplicity and striving to enlighten all settings that are applicable by extension to industrial applications, this study focuses on the SFS2 full scale simulation reference in [1], where *headwind*, *Green 45°* and *Green 90°* conditions, at 40 kts freestream are investigated using both RANS and SBES modelling. From there, being *Green 90°* the most demanding case for simulation accuracy referenced in literature, that setup is re-evaluated with two different models for the Atmospheric Boundary Layer.

3.2. The Atmospheric Boundary Layer

To model the Atmospheric Boundary Layer seems a simple task at first glance. In recent years however its application is becoming of increasing interest in various engineering fields. The need to proper model it, and often to do it in a non-standardized manner, is clear from studies such as [2] and [3] (this

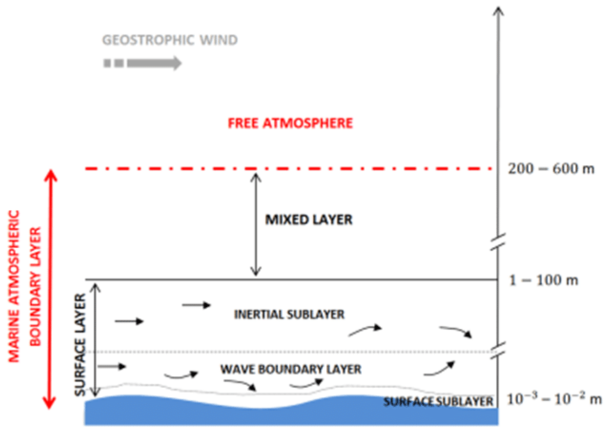

Figure 2: Simplified scheme of ABL at sea

second study incidentally relevant for the other aspect of sea operations for helicopters, namely personnel transport to offshore platforms). In particular in [2] is clearly demonstrated how the assumptions of having one single condition of ABL representing all possible sea states is reductive at least. The approach historically used for rotorcrafts operations should therefore takes these variations into account in the next future, shall *Certification by Simulation* remain an upcoming priority in the industry.

Historically, since the introduction of the *Beaufort Scale* [12] and subsequently the *Douglas Sea Scale* [13], the wind always played a relevant role for naval operations. Naturally, Ship Operations for helicopters are strongly affected as a results, and the turbulence experienced on deck can determine different outcomes, as enlightened in [14].

The output of the aerodynamic analysis is the spatial and temporal distributions of velocity on the ship deck. The analysis will benefit from recent methodological improvements, pushing them even further with the inclusion of the Atmospheric Boundary Layer (ABL). The output of these analyses feeds the aeroelastic simulations, particularly relevant in the startup procedures during the early engine-on phases of ship operations. Indeed, these loads are critical in those phases where rotor blades do not benefit of the centrifugal contribution to stiffness. The excessive blade motions could limit the normal operations on the ship deck because of hard contact forces on blade stops.

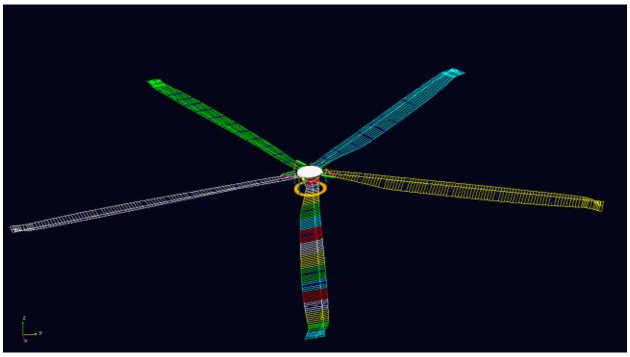

Figure 3: Main rotor aeroelastic model used for start-up manoeuvres analyses

4. AERODYNAMICS METHODOLOGY ESTABLISHMENT PROCESS

4.1. General

The aerodynamic analyses have been carried out by means of finite volumes CFD simulations, exploring diverse possibilities in terms of meshing, numerical schemes, timestep and computational performance. The results have been referenced to the intended function of the data produced, in terms of the effect of the airspeed fluctuations on airloads estimation.

4.2. Computational Domain

A review of the available literature helps to determine guidelines for the domain description. From [4] and [9] appears the need to have a domain where the boundary conditions are imposed at about five times the main dimension of the ship model, since it is the least dimension sizing were the field gradients of the BC imposition are not affecting anymore the flow topology and development. Some studies, such as [10], propose a different approach based on a scaled model, interesting for the SFS2 specific case, which is not completely Reynolds-driven in its methodology (as clarified in [14]), but the limitation in the applicability on other cases makes it irrelevant to the purpose of this study. There is in fact the need to answer a fundamental need in this kind of simulations: the airloads need to be mapped for all possible azimuths of incoming wind, which makes this problem even more comprehensive in terms of computational domain.

Indeed, in the industrial approach to ship operations for helicopters on deck, the investigation must pursue different wind velocities and all possible azimuths, otherwise the helicopters usage clearance would have to be limited. This increases conspicuously the number of simulations required for each aircraft-ship combination. Literature is rich of examples of CFD derived data for piloted simulations; two of the first studies are papers [15] and [16], which led to many other instances of building an entirely simulative environment, which purposes can actually vary.

Since the ultimate objective was to assess a methodology widely applicable, the natural choice for volumetric elements was a fully unstructured mesh. Real life applications of CFD study of ships need to take into account a plethora of possible structures, with various sizes and shapes, and therefore building a structured mesh of sufficient qualities inside the time schedule usually planned in companies is often unfeasible. For the very same reason the choice of triangular surface elements was the simplest one to allow the simulation of arbitrary shaped elements.

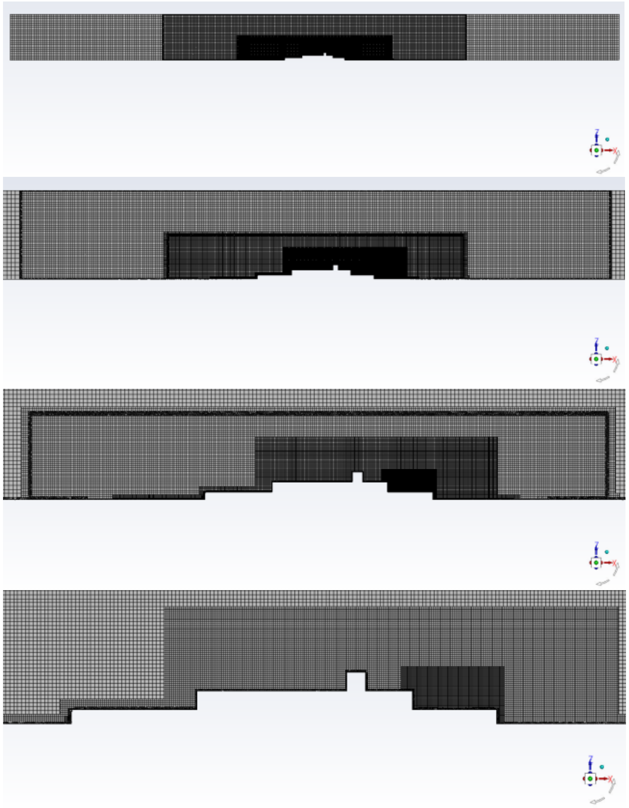

Figure 4: Mesh sectional scheme

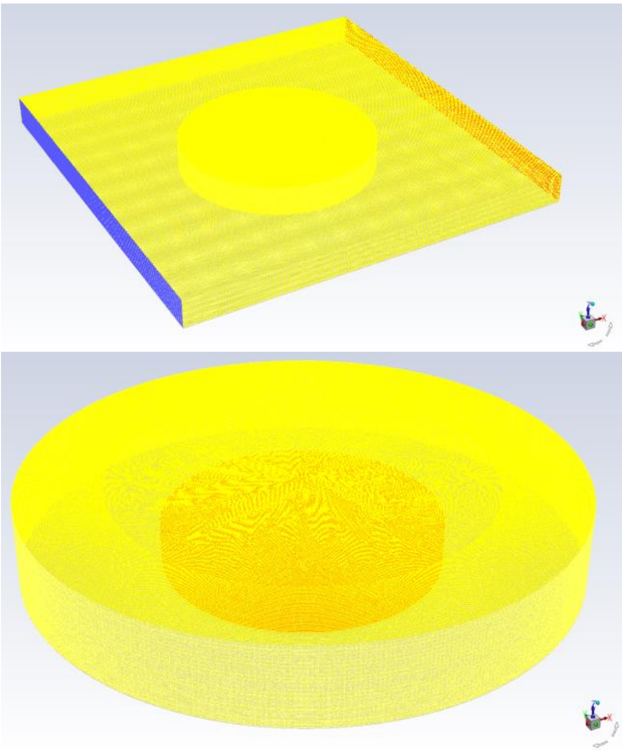

Figure 5: Mesh overview

The basic requirements for an applicable industrial workflow are a domain description as general as possible and a mesh building process applicable to all possible geometries. The same domain shall be built just once, and should be able to adapt to all possible azimuths. The model needs to be efficient also in terms of cell generation, modelling those features that do not affect the solution. The more parts of the domain that can be kept common between different cases, the better. Therefore, the best outcome is a domain of this kind:

- an outer box with side long 5 *Ls* (Ls = length of the ship, in this case 455 [ft]) boxed with a cutcell approach. This box is 0.75 *Ls* tall and holed in the center.
- an inner cylinder of diameter 2.5 *Ls* meshed with hexahedral approach. This cylinder is 0.75 *Ls* tall as well, but has a cut out portion in the lower central region.
- a smaller cylinder inside the first one, 0.375 *Ls* tall and with 1.25 *Ls* diameter, meshed in smaller hexahedral elements enclosing the ship itself and its volumetric prism layers (in red in Figure 5).

The outer box helps the simplification of BCs, keeping the same inlet and the same outlet for all azimuths simulated at the same airspeed. Moreover, splitting the outer mesh helps to save cells using different refinements and allows the analyst to avoid generating different cases of changing anything among different conditions.

In particular, given the possibility to establish non-conformal interfaces in *Ansys Fluent* ©, the azimuth angle can be imposed simply by rotating the outer box with respect to the inner mesh; being extremely light in cell count, the operation is extremely agile and fast to perform. All the outer volume zones can be saved and then reused for all ships of the same class and similar length. This is yet another advantage of such approach.

Furthermore, the subdivision in inner and outer cylinder intrinsically works as a direction-insensitive refinement region, making the mesh once more suited for all-azimuth simulations.

As general rule, per legacy approach, in aerodynamic load estimation the flow field needs to be discretised at over 20 locations per blade radius. For establishing the best CFD setup, a fictional main rotor centered at 5 [m] from the ground and with a 6 [m] main rotor radius was chosen; this would correspond to a 30 [cm] discretised volume region. From there, a refinement box was imposed inside the inner cylinder, right above the aft part of the ship where the helicopter is expected to station on deck.

Such refined region is intended to include all possible motions of the blade during the subsequent aeroelastic analysis, and on the cell zones node the values of x velocity, y velocity and z velocity will be collected to build the wind maps used for the aforementioned coupled simulation.

In order to avoid excessive TVR in the separated zone and to preserve the correct wake structure down to the helicopters location, a refinement box of sizes Ls x Ls/4 x Ls/4 was defined and centered at (Ls/4, 0, Ls/8), being z=0 the sea surface.

In conclusion, the result would look like Figure 4 and Figure 5.

The outer box is the only one with quadrangular faces all around its surfaces and its sides are discretized into 140 cubic cells. With the inner cylindrical hole, the total count of cells for the outer box is 2M elements. This led to a mesh cell count of around ~13M cells.

4.3. Numerical Setup

In terms of boundary conditions, the baseline simulations exploited a no-slip wall boundary condition on the ship surfaces, a slip wall BC on lower and upper surfaces and a pressure inlet / pressure outlet BC setup for the two faces respectively at minimum x-axis and maximum x-axis coordinate of the outer box. To compare properly with available literature results for the SFS2, ISA SL were considered for atmospheric conditions, with a freestream velocity of 40 [kts] – or an expression to match it with the ABL velocity profile. The most relevant azimuth was simulated: *Green 90°*.

The choice of this particular angle comes from the results of aeroelastic analysis presented in [1], as well as the flow pattern analysis in [14].

In particular, it is evident from [2] that for headwind conditions, the flow pattern on deck for a SFS2 ship is weakly related to the ABL modelling introduced. At the same time, from [1] can be gathered that the *Green 90°* condition is the one where the usual models are supposed to work best without ABL.

For these reasons, it is understandable how the ABL velocity gradient could have the highest impact when the superstructures of the ship influence the least the flowfield, and at the same time, we can verify how much the RANS baseline resolution is challenged with respect to the validation in [1].

These setups were common across all simulations.

The necessary first step is to perform a precursor RANS simulation in order to establish a valid initialisation for unsteady cases – and also to have a reference comparison with respect to legacy approach.

4.4. Modelling the ABL

The CFD simulations have been performed exploiting Stress-Blended Eddy Simulations; the modularity in the domain building process allows for an easy implementation of atmospheric boundary layer modelling. The atmospheric boundary layer is an element contributing to the velocity distribution on deck, especially for those azimuths where the wind do not encounter many superstructures (such as 90°). It is in fact a simple introduction in terms of complexity of modelisation, since it does not add degrees of freedom to the system (as it could happen considering hull motions, for instance). In particular, investigating the possible strategies implemented in similar solvers, the first approach followed was an analytical introduction of the mean velocity profile for ABL – from there on, referred to as *ABL-1*.

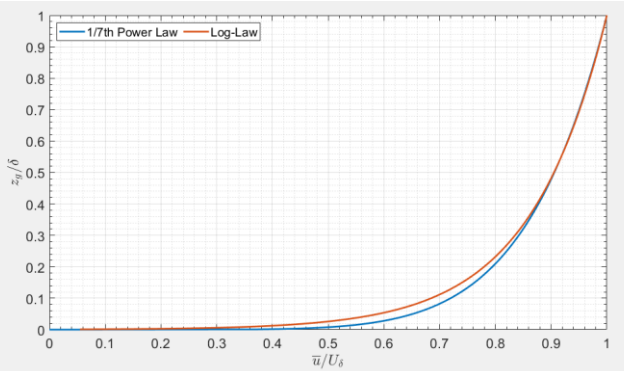

Figure 6: ABL-1 vs ABL-2 analytical profiles

Its imposition on a velocity inlet boundary condition and a slip wall boundary condition for the sea surface is the most canonical approach. The effects of such choice, is then compared to the baseline results in the concluding remarks section.

In particular, this approach exploits the so-called *power law*, that for ABL is often formulated as:

$$\frac{\bar{u}}{U_\delta} = \left(\frac{z_g}{\delta}\right)^n$$

with $n = \frac{1}{7}$ and $U_\delta = 99\%\, U_\infty$, z_g representing the height over SL and $\delta = z(U_\delta)$.

For our case, in order to maintain the same average velocity at the same distance from the sea level, the boundary condition imposed at the inlet is a velocity inlet profile based on the power law.

$$vel_{normal} = 27.1745 \left(\frac{z_{coordinate}}{67.05}\right)^{\frac{1}{7}}$$

The goal was to have at the hub center the same freestream velocity, so calibrating the ABL distribution as to match the 40 kts at the same 5m from deck.

The second approach– hereafter referred to as *ABL-2* – basically consists in exploiting the modularity of the meshing domains to recreate a boundary layer of the expected thickness. This in particular represents an interesting possibility potentially representing a simpler and somewhat comprehensive manner of taking into account the presence of ABL in all possible conditions simulated in a rotor startup procedure applied only within the innermost cylinder of the mesh. Along with that, this could in future unlock the surface roughness as a usable degree of freedom to enhance the ABL representation for different sea states, possibly relating to the experimental correlations expressed in [2]. This would be of simple comparison with respect to the *logarithmic law* that for ABL is usually expressed as:

$$\frac{\overline{u}}{U_\delta} = \frac{\ln\left(\frac{z_g}{z_0}\right)}{\ln\left(\frac{\delta}{z_0}\right)}$$

with z_0 representing the roughness reference length. For a calm sea state, usually it is considered $z_0 = 0.045\ [m]$. That is the reference length considered on the rough wall boundary condition used in the inner cylinder's *minimum z face* (along with a *roughness constant* of 0.5). Combining the log-law ABL model with the sublayer description given by the wall roughness, a better description of turbulent content and low altitude velocity is achieved.

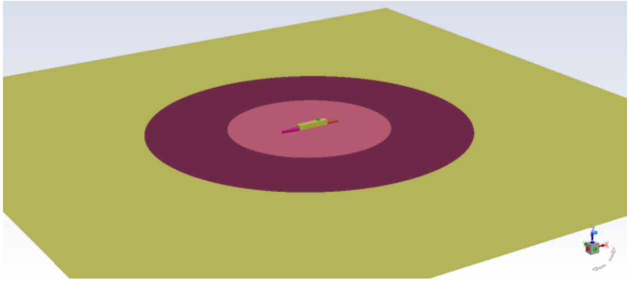

Figure 7: Sea surface discretisation

4.5. Resolution accuracy

Through all simulation setups, the RANS turbulence closure was always operated via kw-sst model, both in precursor or baseline RANS as well as for the unresolved portion of the domain during LES-type simulations (SBES in this case).

The SBES baseline simulations without ABL modelling are carried out with the same setups found in [1].

For a LES-type simulation is important to assess beforehand the amount of TKE that will be properly solved and not modeled via RANS turbulence closure. The main quantity of relevance is the ratio of grid length scale to integral length scale:

$$R_L = \frac{\Delta_{max}}{L_t^{RANS}}$$

$$L_t^{RANS} = \left(\frac{k^{3/2}}{\varepsilon}\right)$$

The higher R_L, the lower resolution is provided to the simulation. (It can be clearly seen from the second formula that a two-equation turbulence method is required to evaluate the grid length scale).

Considering *L* as the smallest resolved eddy scale, and that we need at least a couple cells in each direction to solve it, the main dimension of the cells capturing such a vortex will be: $\Delta = L/2$.

We need to resolve the eddies whose sizes are larger than roughly half the size of the integral length scale, L_0. A good LES practice is to have at least 5

Method	Solver	Time	Pressure	Momentum
RANS	Coupled	-	2nd order	2nd order
SBES	Simplec	Bounded 2nd implicit	2nd order	Bound. C. D.

Table 1: numerical settings

cells across L_0 to resolve 80% of the spectrum.

Once defined the integral length scale, the number of cells per L_0 can be assessed assuming that

$$\Delta = \sqrt[3]{\boldsymbol{Cell_{VOLUME}}}$$

This naturally becomes inaccurate for non-cubic cells. For our domain, where most is covered via hexahedral elements, this is an acceptable assumption.

Steady RANS simulation has been run for 1000 iterations, with an *equivalent* CFL number of 200 with all solvers were set to second-order accuracy in space.

Clipping the contour plot of the L0 over Δ ratio, the coloured zones are the ones where the TKE is under-resolved with respect to the desired target. It is worth noticing that the zone of interest (above the aft deck) was always resolved for the *Green 90°* condition (Figure 8) being cut out of the contoured region of the zx-scanplane.

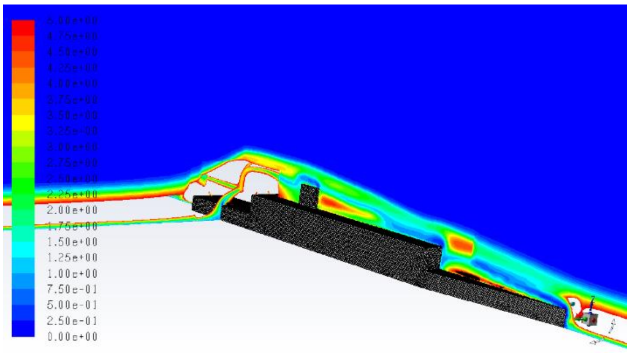

Figure 8: Length ratio contours scheme

In evaluating the best compromise for timestep size, different solutions have been tried.

$$C = \frac{u\Delta t}{\Delta x}$$

Computing a Courant number ≈ 1 value for the zone of interest, namely the rotor refinement box, the resulting timestep was ≈ 0.015[s].

In conclusion, the best approach to time discretisation fitting all simulations featured:

- 1000 iterations in RANS mode
- 2000 iterations at 5x10^{-4} [s] with 20 spatial sub-iterations
- 1000 iterations at 1x10^{-3} [s] with 20 spatial sub-iterations
- 1000 iterations at 1x10^{-3} [s] with 10 spatial sub-iterations
- 30000 iterations at 1x10^{-3} [s] with 10 spatial sub-iterations

Last step is referred to those iterations where the results were acquired to be analysed and compared in terms of frequency content and mean velocity profiles, other than computing the average computional cost. These progression of settings was functional to ensure stability of the solution and a proper convergent trend.

4.6. Performance Analysis

All simulations were performed on the same hardware, in order to be able to compare only the performance advantages given by the model itself, and in a range where both mesh resolutions were still in the linear speedup range of parallel load sharing performance. All simulations were executed on a 480 cores setup, exploiting 48 cores nodes with intel Xeon processors on the *DaVinci-1* cluster located in Genova.

It is straightforward to notice the limited computational cost that the introduction of the *ABL-1* entails on simulations; a very different results with respect to what happens for *ABL-2* model.

The computational time for *ABL-2* is 205% higher with respect to *ABL-1* and 219% higher with respect to the baseline case.

Model	**SBES**	**SBES + ABL-1**	**SBES + ABL-2**
Average wall clock time per iteration [s]	0.387	0.412	0.846

Table 2: computational performance

5. AEROELASTIC ANALYSIS

Aeroelastic simulations are performed by means of a multibody model by means of MSC Adams™ software Main rotor model reproduces the fully nonlinear kinematics of the system along with blade flexibility and its aerodynamics through a panel distribution.

Conditions simulated in this context are transient rotor start up coupled with the wind described by

CFD computed maps; a graphical example of such maps is shown in Figure 9 where Vx, Vy and Vz gain w.r.t. the free stream are depicted. These applied wind maps remain constant during the whole transient run-up of the rotor while the blades move inside this field. The model represents a mid-level coupling between the aerodynamics and the structural analysis, since the rotor motion do not release wake nor modifies the aerodynamic field around. This however is considered a satisfactory hypothesis, since the most critical conditions happen with very low pitch of the blades starting at null translational speed. In such conditions there is almost no lift generation by the rotor disk, and therefore no disk loading.

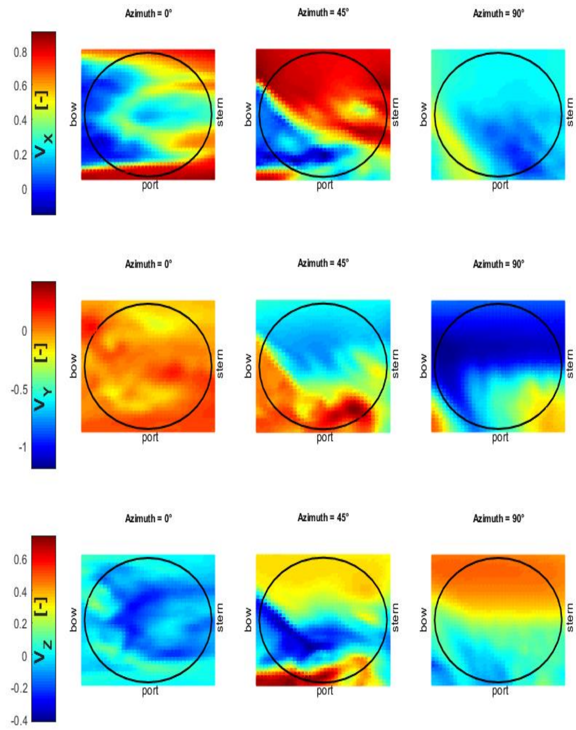

Figure 9: CFD Map example: Vx, Vy and Vz

Usually, the major focus in this kind of analyses is on the out of plane bending of the blade since the centrifugal stiffening effect is not present in the first time instants of the simulation and the blade is free to experience huge flapping motion, sometimes reaching the flap stops with consequent impact.

For these simulation, a realistic rotor model close to the ones used for the AW family, complete with all the hub controls and links, was used in order to have a reliable sensitivity to the outcomes.

6. RESULTS

Using the q-criterion for vorticity, the iso-surfaces in Figure 10 Figure 11 Figure 12 describe the impact of the different flow descriptions: the vortical structures are slightly different, as well as flow phenomenology.

It is thus necessary to focus on the zone of interest; there it can be seen that the baseline case is already sufficient to describe the most important vortical structures, and that in all cases the SBES model is adequately fast in transitioning to LES mode and correctly representing turbulence right after the bluff body separation.

However, the higher turbulent content in ABL-2, due to the surface sublayer description granted by the no-slip rough wall, make the scale of the turbulent structures slightly stabler when the flowfield separates on the deck's edge. It must be noticed that the assumed sea state is naturally of big impact in the ABL-2 modelling, since the roughness reference length is strictly related to the mean wave height, and is a key parameter to determine the surface sublayer of ABL. For this reason, that model would further change the velocity patterns and distribution when others sea states are to be simulated. This would end up giving the expert an additional degree of freedom to use, possibly enhancing the simulation capabilities further on towards certification.

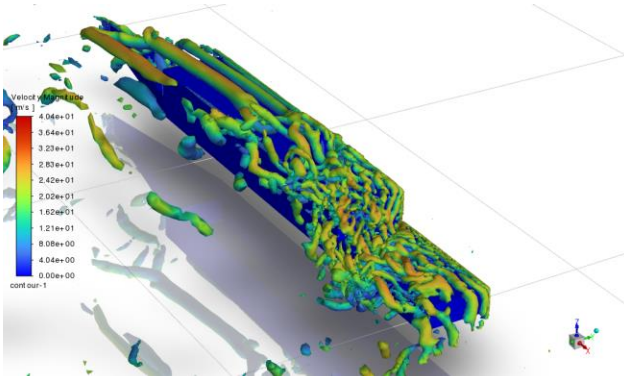

Figure 10: Iso-Q surfaces, baseline

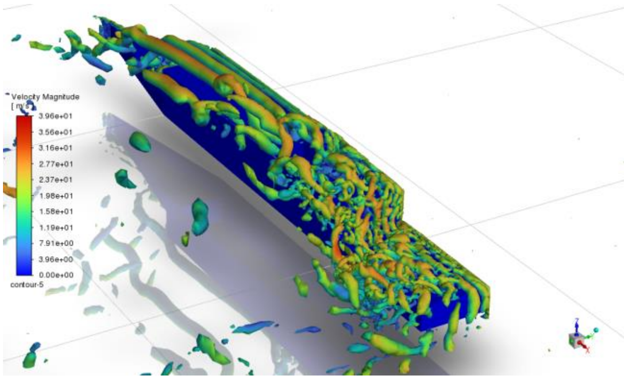

Figure 11: Iso-Q surfaces, ABL-1

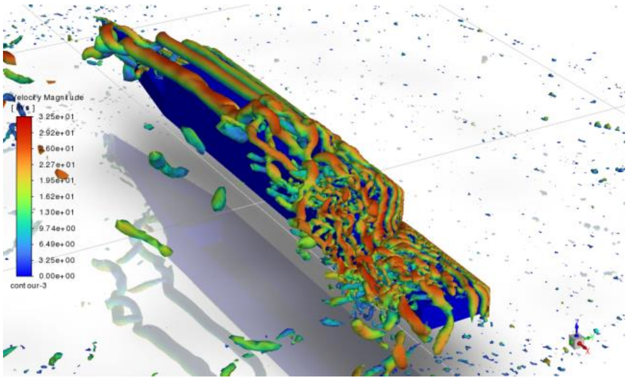

Figure 12: Iso-Q surfaces, ABL-2

Aeroelastic simulations result

Aeroelastic simulations results are presented in this section and are compared with what shown in [1].

From a rotor loads point of view, the most important load component to monitor for this type of condition, characterized by varying RPM under turbulence, is the out of plane blade bending (also referred as beam bending or flatwise bending). For this reason, all figures here presented are associated to such moment for one of the blades and numerical values are adimensionalized with the rotor radius. Aeroelastic simulations are performed for the case with asymptotic wind coming from 90 degree starboard. All graphs show a comparison of the aeroelastic simulations performed considering a wind map generated by the ABL1, ABL2 methods and then SBES analysis from [1] to be taken as reference.

First, Figure 13 shows the beam bending time history during the complete rotor start-up for the simulations mentioned above. Note that the highest bending is obtained when the rotor NR are still low due to low stiffening effect of the centrifugal force while as the NR increases the bending decreases. At first glance, all three aeroelastic simulations present the same behavior and seems that all three wind maps can be considered acceptable for a rotor loads estimation process.

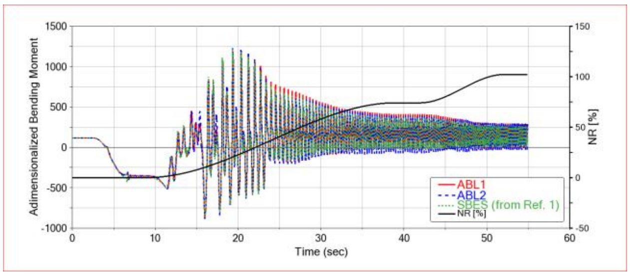

Figure 13: Blade Beam Bending time history during the complete rotor run-up

Figure 14 shows the blade beam bending time history for a stabilized portion of the time history in which the rotor is at its nominal rotational speed, always for the case with the wind direction of 90 deg. In this stabilized period, it is possible to appreciate the differences between the various winds maps considered for this assessment.

Green dotted line is a reference analysis for the loads estimation process and is taken from [1] while the solid red and dashed blue line represent the aeroelastic simulations with new wind map including the ABL effect.

Overall, in all three simulations the rotor out of plane response is similar. ABL2 simulation present a slight different bending trend for the lower load peak, which is anyway close to zero. On the other hand, both ABL runs show an increase for the maximum peak of ~10% w.r.t. the reference simulation with the SBES wind map.

In the context of a loads evaluation process for ship operations it is fundamental to account for all those aspects which can give rise to a load increase and, from these simulations, it emerges that the ABL should be taken into consideration when generating wind maps.

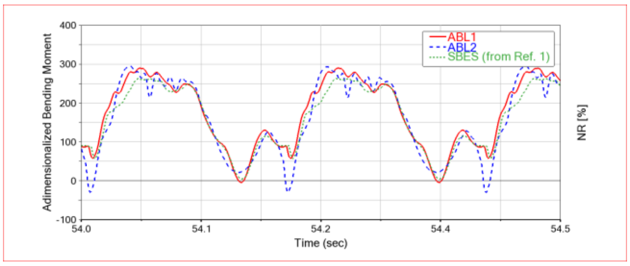

Figure 14: Blade Beam Bending (rotor at nominal rotational speed) – time history

To better comprehend the differences between the two ABL simulations a FFT of the signal shown in Figure 14 is performed and shown in Figure 15. The ABL2 simulation shows, in particular, a higher response at 1/rev and 3/rev and thus the differences present in the time history.

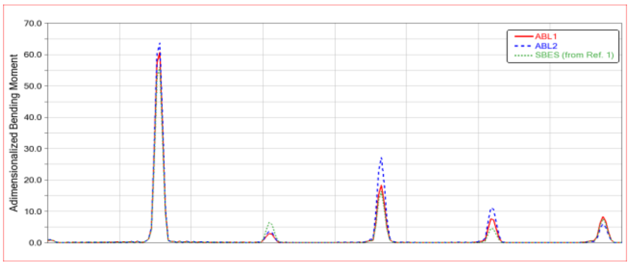

Figure 15: Blade Beam Bending (rotor at nominal rotational speed) - FFT

To summarize, blade beam bending response is evaluated considering a rotor run-up with wind maps coming from CFD simulations performed with ABL-1 and ABL-2 methods. The out of plane dynamic response of the rotor (when spinning at its nominal rate) shows some dependency on the ABL method, in particular the second approach seems to be more severe from a load point of view, anyway peak values are similar in both cases.

An increase in the maximum values is noticed w.r.t. reference simulation that considered a wind map coming from a SBES CFD without accounting for the ABL. It is then important to account for the ABL when going through a load estimation process for ship operations.

Moreover, all these simulations are performed considering a relatively low sea state level (associable to sea state 1-2). The impact of the ABL in the wind map generations might be even more important when considering higher sea state levels typically associated with a limit loads evaluation.

7. CONCLUSIONS

The simulation methodology for rotor loads estimation in ship airwakes comprehensive of atmospheric boundary layer has been investigated in this paper. The outcomes outlines the following best practices:

1. For the most affected condition, with wind coming at 90° on deck, the modelisation of an ABL can sensibly modify the velocity profile reaching the deck.
2. The transient behavior in the bending moment, the peak values and the overall simulation outputs more reliable results and different frequency contents.
3. The utterly dependent behavior of these applications on azimuth and ship geometry discourage the use of simple models for taking into account the aerodynamics of the wake in industrial applications. The reliability of the setup must be tested and verified for all conditions before concluding the best methodology.
4. The vertical gradient of velocity granted by the ABL introduction would have even greater impacts on a SHOL simulation featuring landing or take-off manoeuvres, where the rotors motion envelope is not as limited as in this application.
5. The ABL-2 model, with its higher computational cost, is however the most promising given the possibility to tailor its formulation to different sea-states.

Author contact:

- Gregorio Frassoldati

  gregorio.frassoldati@leonardo.com

- Cristiano Capizzi

  cristiano.capizzi@leonardo.com

8. REFERENCES

Literature references for the present study are listed below in order of citation.

1. Frassoldati, G., Capizzi, C., Prederi, D., and Melone, S., “Coupled Ship Airwake and Rotor Airloads Simulation Methodology,” 49th European Rotorcraft Forum, Bückeburg, Germany, September 5-8, 2023.
2. Liu, C., Li, X., Song J., Zou, Z., Huang, J., Zhang, J. A., Jie, G., and Wang, J., „Characteristics of the Marine Atmospheric Boundary Layer under the Influence of Ocean Surface Waves,“ *Journal of Physical Oceanography*, Vol. 52, June 2022, pp. 1261-1275. DOI: 10.1175/JPO-D-21-0164.1.
3. Larsen, S. E., „The Atmospheric Boundary Layer over Land and Sea: Focus on the Off-Shore Southern Baltic and North Sea Region,“ *DTU Technical Report*, January 2013.
4. Yuan, W., Wall, A., and Lee, R., “Combined numerical and experimental simulations of

unsteady ship airwakes," *Computers and Fluids*, Vol. 172, June 2018, pp. 29-53. DOI: 10.1016/j.compfluid.2018.06.006.

5. Popinet, S., Smith, M., and Stevens, C., "Experimental and numerical study of the turbulence characteristics of air flow around a research vessel," *Journal of Atmospheric and Oceanic Technology*, Vol. 21, (10), 2004, pp. 1574-1589.

6. Kaaria, C. H., Forrest, J. S., Owen, I., and Padfield, G. D., "Simulated aerodynamic loading of an SH-60B helicopter in a ship's airwake," 35th European Rotorcraft Forum, Hamburg, Germany, September 21-25, 2009.

7. Watson, N. A., Owen, I., and White, M. D., "Piloted Flight Simulation of Helicopter Recovery to the Queen Elizabeth Class Aircraft Carrier," *Journal of Aircraft*, Vol. 57, (4), Jul.-Aug. 2020, pp. 742-760. DOI: 10.2514/1.C035733.

8. Sharma, A., Padthe, A., and Friedmann, P. P., "Helicopter Shipboard Landing Simulation Including Wind, Deck Motion and Dynamic Ground Effect," *Journal of Aircraft*, Vol. 58, (3), May-June 2021, pp. 467-486. DOI: 10.2514/1.C035973.

9. Forrest, J. S., and Owen, I., "An investigation of ship airwakes using Detached-Eddy Simulation," *Computers and Fluids*, Vol. 39, November 2009, pp. 656-673. DOI: 10.1016/j.compfluid.2009.11.002.

10. Shukla, S., Singh, S. N., Sinha, S. S., and Vijayakumar, R., "An Investigation of Ship Airwakes by Scale Adaptive Simulation," *the International Journal on Marine Navigation and Safety of Sea Transportation*, Vol. 14, (2), June 2020, pp. 471-475. DOI: 10.12716/1001.14.02.27.

11. Thornber, B., Starr, M., and Drikakis, D., "Implicit Large Eddy Simulation of Ship Airwakes," *Aeronautical Journal*, Vol. 114, (112), 2010, pp. 715-736.

12. Saucier, W. J., „Principles of Meteorological Analysis," *The University of Chicago Press*, 1955.

13. Owens, E. H., and Schwartz, M. „Beaches and Coastal Geology," *Encyclopedia of Earth Sciences Series*, September 1984, p. 722. DOI:10.1007/0-387-30843-1_397

14. Seth, D., Leishman, J. G., Gnanamanickam, E., and Zhang, Z., "Time-Resolved Ship Airwake Measurements in a Simulated Atmospheric Boundary Layer," *Journal of Aircraft*, Vol. 58, (3), May-June 2021, pp. 624–649. DOI: 10.2514/1.C035886.

15. Forrest, J. S., Hodge, S. J., Owen, I., and Padfield, G. D., "An investigation of ship airwake phenomena using time-accurate CFD and piloted helicopter flight simulation," 34th European Rotorcraft Forum, Liverpool, UK, September 16-19, 2008.

16. Hodge, S. J., Zan, S. J., Roper, D. M., Padfield, G. D., and Owen, I., "Time-Accurate Ship Airwake and Unsteady Aerodynamic Loads Modelling for Maritime Helicopter Simulation," *Journal of the American Helicopter Society*, Vol. 54, April 2009, pp.1-16. DOI: 10.4050/JAHS.54.022005.